

GENERALIZED MATHEMATICAL HOMOGENIZATION OF THE LATTICE DISCRETE PARTICLE MODEL

ROOZBEH REZAKHANI*, GIANLUCA CUSATIS†

*Northwestern University CEE Department
2145 N Sheridan Rd, Evanston, IL 60208, USA
e-mail: rrezakhani@u.northwestern.edu

†Northwestern University CEE Department
2145 N Sheridan Rd, Evanston, IL 60208, USA
e-mail: g-cusatis@northwestern.edu, www.cusatis.us

Key words: Discrete Models, Mathematical Homogenization, Micro-Polar Continuum, Asymptotic Expansion

Abstract. Concrete, ceramics, fiber and particle reinforced composites, as well as porous media, are materials widely used in industry and engineering. All these materials are heterogeneous at a certain scale and some of their specific macroscopic behaviors during damage can be traced back to their micro structural behavior. In order to obtain realistic results in the numerical simulations of heterogeneous materials, one needs either to perform computationally intensive fine scale simulations or to adopt a multi-scale technique that is able to reduce the computational cost of the analysis while it retains enough accuracy on the quantities of interest. In this paper the mathematical homogenization approach is used to upscale the Lattice Discrete Particle Model (LDPM), that have been successfully formulated to simulate concrete at the scale of the major heterogeneities. The Lattice Discrete Particle Model (LDPM) simulates concrete at the meso-scale considered to be the length scale of coarse particle pieces. Contrarily to continuum-based approaches, in discrete models like LDPM, the displacement and rotation fields are only defined in a finite number of points representing the center of coarse aggregate particles. The mechanical interaction between adjacent particles is governed by meso-scale constitutive equations. In this work LDPM is homogenized through the classical mathematical homogenization by employing first order asymptotic expansions for displacements and rotations. Numerical simulations are carried out to analyze the behavior of the resulting homogenized macroscopic constitutive equation.

1 INTRODUCTION

Most of natural and engineering materials, such as ceramics, concrete, composites and rock are heterogeneous at some scale. This heterogeneity at lower scales is the root of a variety of macroscopic behaviors, especially during failure. Experiments show that governing behavior of heterogeneous materials strongly rely upon the characteristics of heterogene-

ity, such as, but not limited to, size, spatial distribution, and shape. Therefore, to capture the realistic global behavior of heterogeneous materials, a multi scale analysis of material is inevitable. Among different multi scale techniques, homogenization is a well known method widely used over the past decades. Eshelby [1] and Hashin and Strikman [2] were among the first to develop analytical homogenization techniques for the analysis of compos-

ite materials. Analytical homogenization techniques provide reasonably approximate material properties in the elastic regime but they become prohibitive to apply when nonlinear effects need to be accounted for. by mathematically solving a boundary value problem. Nonlinear problems characterize by plasticity and strain hardening have been solved in the past decade through the so called computational homogenization (see Refs. [4] to [7]), in which the gauss point response of a given material is obtained by applying appropriate boundary conditions to a representative volume element (RVE). The RVE, firstly introduced by Hill [3], is defined as a the smallest volume of material in which heterogeneous structure is explicitly modeled and whose homogenized response is statistically insensitive to the fine features of the material internal structure. Since no assumption is made for the macroscopic constitutive law, this method can be used for extremely nonlinear material behaviors.

Another type of homogenization technique, called Asymptotic Expansion Homogenization (AEH), uses asymptotic expansion of displacement field to build the homogenization framework. The asymptotic expansion is based on a length parameter which is the ratio between an intrinsic size of heterogeneity to a macroscopic typical length. Starting from equilibrium equation and using a variational approach, one can obtain separate governing equations for different scales. By using this approach, one can gain macroscopic average constitutive behavior as well as local distribution of stress and strain fields in the fine scale domain. Chung [8] presented detailed derivation of multiple scale formulation for elastic solids. Fish [9, 10] employed this approach to study linear and nonlinear behavior of composites in a FEM analysis. Ghosh [11] used this approach along with Voronoi Cell Finite Element Method (VCFEM) to study the elastic behavior of composites with random meso-structure as well as elastic-plastic behavior of heterogeneous materials [12]. Fish [13] also used asymptotic homogenization to derive continuum equations

starting from Molecular Dynamic (MD) equations.

Absolute size of the heterogeneity influences the homogenized behavior of a multi phase materials and composites. Classical homogenization techniques described above can take into account the effect of shape and volume fraction of heterogeneity, but cannot capture the effect of absolute size of heterogeneity. In addition, for materials which shows softening behavior, mesh dependency has been a well known problem. To overcome this difficulties, different non-local techniques has been proposed. Modelling materials as Cosserat continua is one of those approaches. Feyel [14] built a homogenization scheme in a FE^2 framework to derive Cosserat continua at macro scale from Cauchy heterogeneous continua at the micro-scale. Asymptotic homogenization technique was also employed by Forest [15] for elastic Cosserat solids. He studied different type of expansion series for displacement and rotation fields and investigated their effect. He showed that the nature of homogenized continua depends on the ratio of the Cosserat characteristic length of constituents, size of heterogeneity and typical size of the structure. Sluis [16] homogenized a RVE of polymer to a Cosserat continua to solve mesh dependency problem of softening materials. In most of the research in homogenization of Cosserat media, fine and coarse scale problems are both considered to be governed by continuum mechanics. The literature is scarce as far as multiple scale homogenization in which fine scale problems are governed by discrete mechanics. Among very few others, recently, Li [17] developed a micro-macro homogenization framework for particulate media.

In this paper, we develop a mathematical scheme to homogenize the Lattice Discrete Particle Model (LDPM), a discrete model for concrete, to a continuum one. LDPM developed by Cusatis et al. [18, 19] is a discrete model that showed an outstanding ability to simulate concrete behavior under a wide variety of loading conditions.

2 The Discrete Fine-Scale Problem

Discrete fine-scale modelling of heterogeneous quasi-brittle materials, including, but not limited to, concrete, rock, sea-ice, toughened ceramics, and composites, has become widely popular during the past few decades due to its intrinsic ability to simulate material heterogeneity and fracture induced displacement discontinuity. Discrete fine-scale models are characterized by the following features: (1) The geometry of the computational model is built with reference to the actual internal structure the material of interest and it consist of “particles” connected through either “contact points” or “connecting struts”; (2) The kinematic description (displacement and rotation fields) are defined only at a finite number of points coinciding with the particle centers; (3) Strain and stress measures are defined only at the contact points or at the centroid of the connecting strut cross sections; (4) Discrete models employ vectorial, as opposed to tensorial, stress versus strain relationships to describe the constitutive behavior; and (5) The classical concepts of equilibrium and compatibility are formulated through algebraic equations, as opposed to partial differential equations typical of continuum mechanics. These characteristics has been proven to be very effective for the realistic simulation of strain localization, fracture, and fragmentation of several different materials.

Classical discrete models are the Discrete El-

ement Method (DEM) and frame/truss models. DEM was first proposed by Cundall [20] to simulate particulate geomaterials, and it has been extensively and successfully used by many authors to model sand, cohesive and cohesive-less soils, and rocks [21, 22]. Lattice models, originally developed by Hrennikoff [23] to solve elasticity problems, were later used by Burt and Dougill [24] to simulate progressive failure in heterogeneous materials. In these models, a network of lattices are used to simulate the discreteness of the meso-structure. Lattice models have been also used to model failure in concrete and composites (see Refs. from [25] to [29]).

If one limits the analysis to the case of small strains and displacements – which is a reasonable assumption in absence of large plastic deformation prior to fracture as observed in brittle and quasi-brittle materials – the fine-scale problem can be formulated with reference to the initial configuration of each single particle (or lattice node) surrounded by a number of neighboring particles (or lattice nodes) as shown in Fig. 1. The basic geometrical entities used to formulate the fine-scale framework are (1) particle centers or lattice nodes – referred as simply “node” thereafter – where displacements and rotations are defined; and (2) the “facets” which represents weak locations in the material internal structures where damage is likely to localize and fracture to occur and where measures of deformation are introduced and constitutive equations enforced.

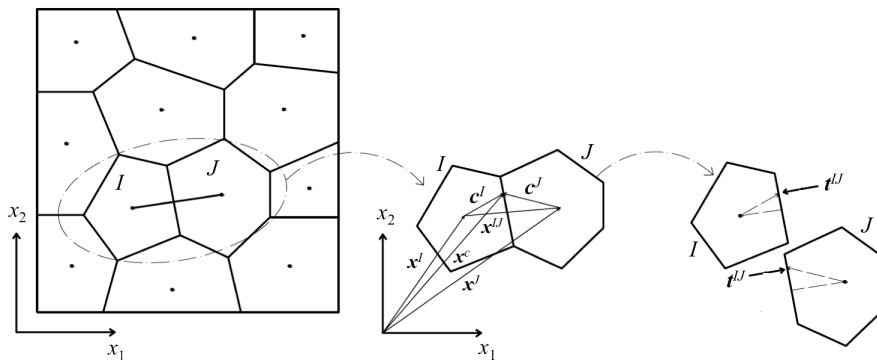


Figure 1: Geometrical vectors in two dimension

Displacement jump on a generic facet f between node I and node J can be written as

$$\llbracket \mathbf{u}_C \rrbracket = \mathbf{U}^J + \Theta^J \times \mathbf{c}_f^J - \mathbf{U}^I - \Theta^I \times \mathbf{c}_f^I \quad (1)$$

Next, measures of deformation can be defined as

$$\epsilon_{f\alpha} = r^{-1} \llbracket \mathbf{u}_C \rrbracket \cdot \mathbf{e}_{f\alpha}^{IJ} \quad (2)$$

where $\epsilon_{f\alpha}$ = strains; $r = |\mathbf{r}^{IJ}|$; $\mathbf{r}^{IJ} = \mathbf{x}^J - \mathbf{x}^I$; $\mathbf{e}_{f\alpha}^{IJ}$ ($\alpha = N, M, L$) are unit vectors defining a facet Cartesian system of reference such that \mathbf{e}_{fN}^{IJ} is orthogonal to the facet and $\mathbf{e}_{fN}^{IJ} \cdot \mathbf{r}^{IJ} > 0$; $\mathbf{U}^I, \mathbf{U}^J$ = displacement vectors of node I and J ; Θ^I, Θ^J = rotation vectors of node I and J ; and $\mathbf{c}_f^I, \mathbf{c}_f^J$ = vectors connecting nodes I and J to the facet centroid. It must be observed here that, in general, displacements and rotations are assumed to be independent variables. Also, curvature type measures of deformation could be included as well but they are not considered here because they are not used in the LDPM formulation.

For a given strain vector, a vectorial constitutive equation provide the stress stress, \mathbf{t}_f^{IJ} , on the facet. Formally one can write $\mathbf{t}_f^{IJ} = t_{f\alpha}(\epsilon_{fN}, \epsilon_{fM}, \epsilon_{fL}) \mathbf{e}_{f\alpha}^{IJ}$ where summation rule applies. As an example, elastic behavior can be formulated through the following equations

$$t_{f\alpha} = E_\alpha \epsilon_{f\alpha} \quad (3)$$

In the previous equations each traction component is proportional to the associated strain (summation rule does not apply); and E_α are fine-scale elastic constants.

Finally, the computational discrete fine-scale framework is completed by imposing the equilibrium of each single particle subject to the effect of all surrounding particles. Translational and rotational equilibrium equations for quasi-static loading conditions read

$$\sum_{f=1}^{N_f^I} A_f \mathbf{t}_f^{IJ}(\epsilon_{f\alpha}) = 0 \quad (4)$$

and

$$\sum_{f=1}^{N_f^I} A_f \mathbf{c}_f^I \times \mathbf{t}_f^{IJ}(\epsilon_{f\alpha}) = 0 \quad (5)$$

where N_f^I = number of facets surrounding node I ; A_f^I = facet area. In all above equations, variables with subscript f are variables related to a specific facet, f , common between the two particles I and J . Hereafter, subscript f is dropped from the equations for simplicity.

3 Mathematical Homogenization Based on Asymptotic Expansion Series

In this section, two-scale homogenization of the general fine-scale problem introduced in the previous section is pursued by means of the generalized mathematical homogenization (GMH), first introduced in Ref. [13] for the multiscale analysis of atomistic periodic systems. In the original formulation only central forces were assumed to act on the particles and, consequently, the rotational equilibrium equation was not considered. This limitation is removed in the current study.

3.1 Two Scale Approximation and Asymptotic Expansions

In order to perform a two-scale asymptotic homogenization, one needs to define two separate scales and the corresponding coordinate systems \mathbf{x} and \mathbf{y} : \mathbf{x} represents the macroscopic coordinate system in which the problem is defined as continuous and it does not see any material heterogeneity; \mathbf{y} is the meso-scale (stretched) coordinate system, in which heterogeneity is modeled by the discrete meso-scale model. If the separation of scales exists, one can write the following relationship linking macro and meso coordinate systems

$$\mathbf{x} = \eta \mathbf{y} \quad 0 < \eta \ll 1 \quad (6)$$

where η is a very small positive scalar. In addition, the displacement of a generic node I , $\mathbf{U}^I = \mathbf{u}(\mathbf{x}^I, \mathbf{y}^I)$, can be approximated by means of the following asymptotic expansion

$$\mathbf{u}(\mathbf{x}, \mathbf{y}) \approx \mathbf{u}^0(\mathbf{x}, \mathbf{y}) + \eta \mathbf{u}^1(\mathbf{x}, \mathbf{y}) \quad (7)$$

where \mathbf{u}^0 is the macroscopic displacement field. Whereas \mathbf{u}^1 is the meso-scale correction which depends on both coordinate systems.

Similarly, the asymptotic expansion of the rotation of a generic node I , $\Theta^I = \theta(\mathbf{x}^I, \mathbf{y}^I)$, can be approximated by the following expansion

$$\theta(\mathbf{x}, \mathbf{y}) \approx \eta^{-1}\theta^{-1}(\mathbf{x}, \mathbf{y}) + \theta^0(\mathbf{x}, \mathbf{y}) + \eta\theta^1(\mathbf{x}, \mathbf{y}) \quad (8)$$

where θ^{-1} is the macroscopic rotation field, θ^0 is a combination of macro scale and fine scale rotations, and θ^1 is the fine scale rotation field dependent on both coordinate systems. Note that in all previous equations and in the rest of this paper, the time dependence of the variable is dropped in the notation for a better readability of the equations. In the macroscopic coordinate \mathbf{x} , the difference in position between node I and J can be considered as infinitesimal. Hence, in order to obtain the asymptotic expansion of strain, it is convenient first to obtain the Taylor series expansion of displacement and rotation at node J around the point I . By assuming that the displacement and rotation fields in Eqs. 7 and 8, are continuous and differentiable with respect to \mathbf{x} , one can write the displacement and rotation of node J as

$$\begin{aligned} U_i^J &= U_i(x_i^J, y_i^J, t) = \\ &= u_i^J + \frac{\partial u_i^J}{\partial x_m} x_m^{IJ} + \frac{1}{2} \frac{\partial^2 u_i^J}{\partial x_m \partial x_n} x_m^{IJ} x_n^{IJ} + \dots \end{aligned} \quad (9)$$

$$\begin{aligned} \Theta_i^J &= \Theta_i(x_i^J, y_i^J, t) = \\ &= \theta_i^J + \frac{\partial \theta_i^J}{\partial x_m} x_m^{IJ} + \frac{1}{2} \frac{\partial^2 \theta_i^J}{\partial x_m \partial x_n} x_m^{IJ} x_n^{IJ} + \dots \end{aligned} \quad (10)$$

where $u_i^J = u_i(\mathbf{x}^I, \mathbf{y}^J)$; $\theta_i^J = \theta_i(\mathbf{x}^I, \mathbf{y}^J)$; x_j^J is a vector connecting node I to node J in \mathbf{x} space. One should replace Eqs. 9 and 10 along with asymptotic expansions of rotation and displacement, Eqs. 7 and 8 into the definition of strain, Eq. 2, to have multiple scale expression facet strain. By doing so and some mathematical manipulations, one gets following form of equations for facet strain

$$\epsilon_\alpha = \epsilon_\alpha^0 + \eta \epsilon_\alpha^1 \quad (11)$$

where

$$\begin{aligned} \epsilon_\alpha^0 &= \bar{r}^{-1} \left[u_i^{1J} - u_i^{1I} + \varepsilon_{ijk} \omega_j^{0J} \bar{c}_k^J - \varepsilon_{ijk} \omega_j^{0I} \bar{c}_k^I \right. \\ &\quad \left. + v_{i,j}^0 y_j^{IJ} - \varepsilon_{ijk} \phi_j^0 y_k^{IJ} \right] e_{\alpha i}^{IJ} \end{aligned} \quad (12)$$

where θ^0 is the sum of ω^0 and ϕ^0 . ϵ_α^1 is a function of asymptotic displacement and rotation terms.

In the above equations variables with a bar sign are length variables in \mathbf{y} coordinate system which are related to the same variables in the \mathbf{x} coordinate system through Eq. 6.

Before proceeding with the derivation, rescaling of the discrete equilibrium equations needs to be performed, in order to obtain the correct scale separation of the governing equations. By dividing Eq. 4 by η^2 , and considering that all length variables should be considered $\sim O(\eta^1)$, one obtains

$$\sum_{J=1}^{N_J^I} \bar{A}^{IJ} \bar{\mathbf{t}}^{IJ}(\epsilon_\alpha) = 0 \quad (13)$$

$\bar{A}^{IJ} = A^{IJ}/\eta^2$ and $\bar{\mathbf{t}}^{IJ} = \mathbf{t}^{IJ}$ are all quantities $\sim O(\eta^0)$.

Similarly, one can also rescale the rotational equation of motion in Eq. 5

$$\sum_{J=1}^{N_J^I} \bar{A}^{IJ} (\bar{\mathbf{c}}^I \times \bar{\mathbf{t}}^{IJ}(\epsilon_\alpha)) = 0 \quad (14)$$

where $\bar{\mathbf{c}}^I = \mathbf{c}^I/\eta$. Also, if one should uses the Taylor expansion for facet traction vector, one can write.

$$\bar{t}_i^{IJ}(\epsilon_\alpha) \simeq \bar{t}_i^{IJ}(\epsilon_\alpha^0) + \frac{\partial \bar{t}_i^{IJ}}{\partial \epsilon_\alpha^0} \eta \epsilon_\alpha^1 \quad (15)$$

Finally, by replacing the above equations in Eqs. 13 and 14, and collecting the terms of $O(\eta^0)$ and $O(\eta^1)$, the multiple-scale equilibrium equations can be obtained as discussed in the next section.

3.2 Fine Scale Governing Equations

One can first consider the terms of $O(\eta^0)$ and scale all terms back

$$\sum_{J=1}^{N_J^I} A^{IJ} t_i^{IJ}(\epsilon_\alpha^0) = 0 \quad (16)$$

$$\sum_{J=1}^{N_J^I} A^{IJ} (\varepsilon_{ijk} c_j^I t_k^{IJ}(\epsilon_\alpha^0)) = 0 \quad (17)$$

These equations are the fine scale equilibrium equations for a single particle placed inside the RVE. Eq. 16 is the force and Eq. 17 is the moment equilibrium equations for particle I . If one consider the definition of ϵ_α^0 , Eq. 12, it can be noticed that there are macroscopic terms which are projected on each facet. The term $v_{i,j}^0 - \varepsilon_{ijk} \phi_j^0$ corresponds to macroscopic definition of Cosserat strain tensor. This macroscopic quantity is transferred from macro scale problem to the fine scale problem and are used as the applied load in the RVE problem to obtain fine scale solution.

3.3 Macro Scale Governing Equations

Now, let's consider consider the $O(\eta^1)$ equations

$$\sum_{J=1}^{N_J^I} A^{IJ} \frac{\partial t_i^{IJ}}{\partial \epsilon_\alpha^0} \epsilon_\alpha^1 = 0 \quad (18)$$

$$\sum_{J=1}^{N_J^I} A^{IJ} \varepsilon_{ijk} c_j^I \frac{\partial t_k^{IJ}}{\partial \epsilon_\alpha^0} \epsilon_\alpha^1 = 0 \quad (19)$$

It can be demonstrated that after some mathematical manipulations, the above macroscopic equations can be expressed as

$$\begin{aligned} \nabla_x \cdot \boldsymbol{\sigma} &= 0 \\ \boldsymbol{\sigma} &= \frac{1}{2V_0} \sum_I \sum_{J=1}^{N_J^I} A^{IJ} (\mathbf{x}^{IJ} \otimes \mathbf{t}^{IJ}) \end{aligned} \quad (20)$$

and

$$\begin{aligned} \boldsymbol{\varepsilon} : \boldsymbol{\sigma} + \nabla_x \cdot \boldsymbol{\mu} &= 0 \\ \boldsymbol{\mu} &= \frac{1}{2V_0} \sum_I \sum_{J=1}^{n_J^I} A^{IJ} (\mathbf{x}^{IJ} \otimes (\mathbf{c}^I \times \mathbf{t}^{IJ})) \end{aligned} \quad (21)$$

where $\boldsymbol{\sigma}$ is the macroscopic stress tensor and $\boldsymbol{\mu}$ is the macroscopic moment stress tensor. These tensors are calculated based on the fine scale solution quantities, \mathbf{t}^{IJ} obtained from solution of fine scale problem, and fine scale geometrical vectors \mathbf{c}^I and \mathbf{x}^{IJ} .

4 Numerical Results

In this section some numerical examples are presented to check the validity of the derived formulation. As mentioned in the previous sections, the Lattice Discrete Particle Model (LDPM) is used in the numerical examples.

4.1 Elastic RVE Analysis

In this section, effective elastic material properties of a representative volume of concrete modeled by LDPM is studied. To carry out the elastic analysis, RVEs of six different sizes are considered: 10, 15, 20, 25, 35, 50 and 100 mm. maximum particle size is chosen as 8 mm. For discrete model parameters, $E_N = 60273$ MPa and $E_M = E_L = 0.25E_N$ are used. Five different particle configurations are considered for each RVE size, and elastic material properties are calculated for all of them.

4.1.1 Pure tension test

To evaluate the Young modulus, a uni-axial macroscopic strain tensor is applied the RVE. All components of the macroscopic strain tensor are zero except for the normal strain in one direction. The RVE problem subjected to this strain tensor is solved, and stress and moment stress tensors are calculated based on the Eqs. 20 and 21. By interpreting the results through classical elasticity, one can calculate Young modulus and Poisson's ratio of the RVE. Figure 2 shows the change in averaged Young modulus and Poisson's ratio with respect to RVE size. Length of the error bars at each size is twice the standard deviation calculated over the five different realization for each RVE size.

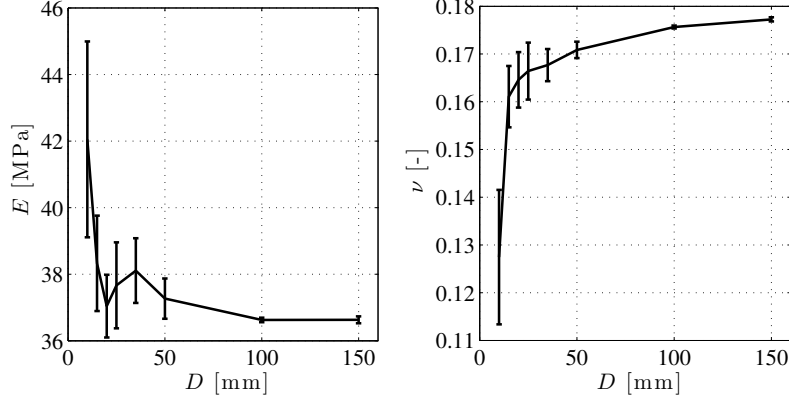


Figure 2: (left) Young modulus and (right) Poisson's ratio evaluated through homogenization and comparison with theoretical formulation

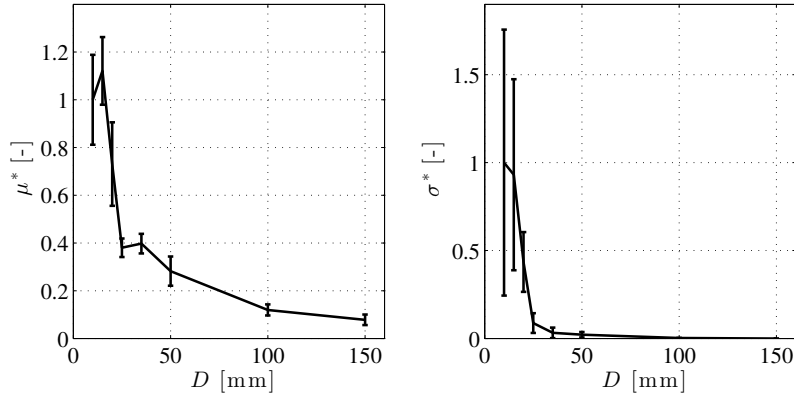


Figure 3: (left) Variation of anti-symmetric part of stress tensor (right) moment stress tensor magnitude normalized with respect 10 mm RVE

One can see that both Young modulus and Poisson's ratio are converging to a constant value by increasing the size of the RVE. Standard deviation of those quantities also tends to zero as size of the RVE is increased. This means that the bigger the size chosen for RVE, the less the particle distribution inside the RVE affects the results.

4.1.2 Simple shear test

The Cosserat character of LDPM is analyzed in this section where a pure shear strain state is applied to the RVE. Moment stress tensor and anti-symmetric part of the stress tensor are the quantities considered here. To investigate the effect of the size of the RVE on these quanti-

ties, the following variables are defined

$$\mu^* = \frac{\sqrt{[\sum_i \sum_j \mu_{ij}^2]_D}}{\sqrt{[\sum_i \sum_j \mu_{ij}^2]_{10}}} \quad (22)$$

$$\sigma^* = \frac{[\sigma_{21} - \sigma_{12}]_D}{[\sigma_{21} - \sigma_{12}]_{10}} \quad (23)$$

with reference to the 10 mm size RVE. Variation of 22 and 23 with respect to RVE size is plotted in figure 3.

The plot shows that increasing the size of the RVE, while the maximum particle size is kept constant, the behavior of the homogenized continuum transition from Cosserat-type to Cauchy-type as demonstrated by the decrease of the magnitude of moment stress tensor and

anti-symmetric part of stress tensor. It means as one increases size of the RVE, medium of interest goes from Cosserat continuum to Cauchy. One can also notice that standard deviation of these quantities also tends to zero by increasing the size of the RVE, which means that mesh configuration is less influential.

4.2 Nonlinear RVE Analysis

In this section, the nonlinear response of RVEs of different size is investigated. RVE sizes of 25, 50, and 100 mm are considered in

this section. Seven different type of mesh configuration (particle distribution inside RVE) is considered for each case. Particle distribution and geometry of one sample of each RVE size is shown in figure 4. Boundary particles are eliminated to be able to show the particles of different sizes inside RVE. Uniaxial strain tensor is imposed on the RVEs, while periodic boundary conditions are applied. Stress-Strain curve are obtained for each RVE and for each mesh configuration.

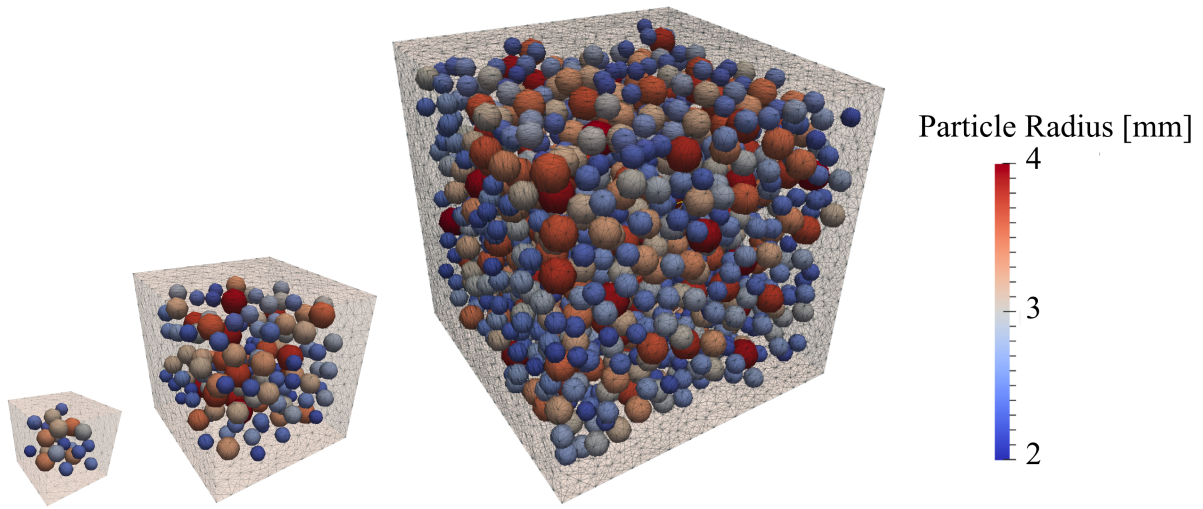


Figure 4: RVE geometry and particle distribution. (left) 25 mm - (middle) 50 mm - (right) 100 mm

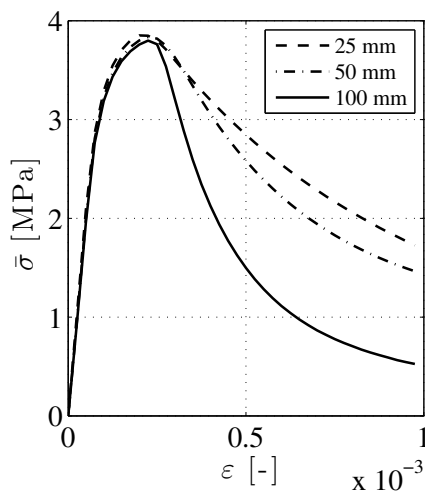


Figure 5: Average tensile stress-strain curve for three different RVE size

The average stress-strain curves are calculated for each RVE size and presented in Fig. 5. It is shown that increasing size of the RVE, forces the post peak curve becomes steeper. This is consistent with the fact that the homogenization procedure can capture strain localization as shown in Figure 6, where one can see the damaged RVEs at the end of tensile loading process. Contours in Figure 6 represent crack opening distributions for an imposed macroscopic strain equal to 0.001. While the ability of the homogenized procedure to handle damage localization is certainly a sign that the procedure captures well the overall behavior of the fine-scale model, it leaves open the question on how to select the size of the RVE. Similar to the work of Gitman and coworkers [30] in the

contest of computational homogenization, the current results suggest that objectivity of the macroscopic response under softening regime

is preserved only if the volume of the RVE is equal to the macroscopic volume associated with the gauss point where the RVE is solved.

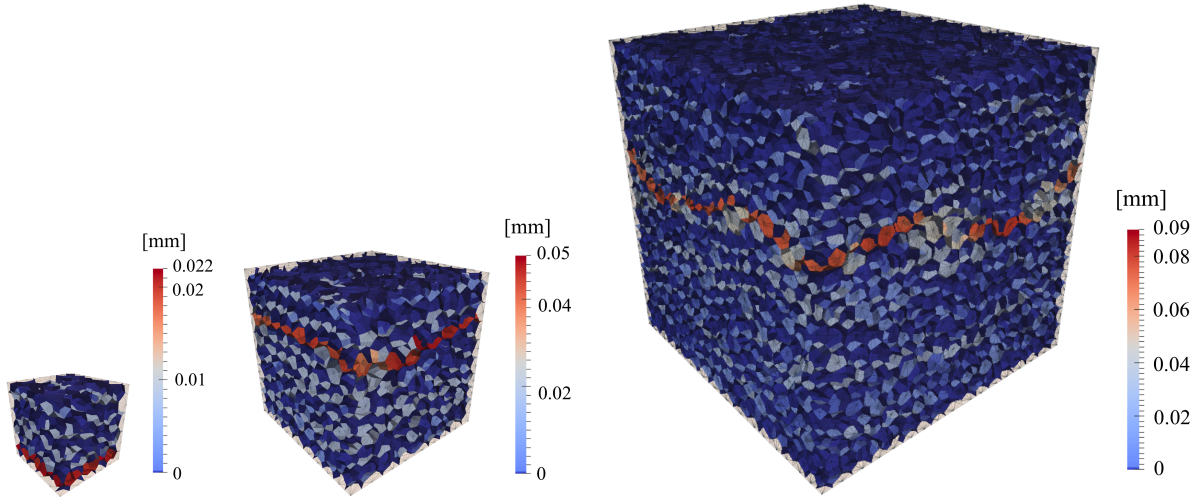


Figure 6: Crack opening contour of damaged RVEs at tensile strain equal to 0.001 (left) 25 mm (middle) 50 mm (right) 100 mm

5 CONCLUSIONS

IN this paper, a mathematical homogenization framework based on the asymptotic expansion of displacement and rotation fields are built starting from the equilibrium equations of motion. Multiple scale formulation for fine scale and macro scale problem are derived. Some linear and nonlinear numerical tests have been carried out on the unit cell and following conclusions are drawn

1. Macroscopic Cosserat strain tensor is obtained as the quantity which should be transferred from macro scale problem to lower scale one as the applied strain.
2. Increasing the size of the RVE, mesh configuration effect on elastic material properties decreases.
3. Increasing the size of the RVE and keeping the maximum particle size constant, Young modulus and Poisson's ratio converges to a constant value.
4. In elastic regime, changing the size of the RVE does not affect the result, while in

the softening regime it influences the results significantly due to damage localization.

5. Due to strain localization happening in the post peak regime, RVE behavior is size dependent, which shows the main problem in homogenization of quasi-brittle materials.

REFERENCES

- [1] Eshelby, J.D., 1958. The determination of the elastic field of an ellipsoidal inclusion and related problems. *Proc. R. Soc. London*. **241A**:376-396.
- [2] Hashin, Z. and Strikman, S., 1963. A variational approach to the theory of the elastic behavior of multiphase materials. *J. Mech. Phys. Solids*. **11**:127-140.
- [3] Hil, R., 1963. Elastic properties of reinforced solids: some theoretical principles. *J Mech Phys Solids*. **11**:357-72.
- [4] Smit, R.J.M., Brekelmans, W.A.M. and Meijer. H.E.H., 1998. Prediction of the

- mechanical behavior of nonlinear heterogeneous systems by multi-level finite element modeling. *Computer Methods in Applied Mechanics and Engineering*. **155**:181-192.
- [5] Feyel, F., 2003. A multilevel finite element method (fe2) to describe the response of highly non-linear structures using generalized continua. *Comput. Methods Appl. Mech. Engrg.* **192**:3233-3244.
- [6] Kouznetsova, V., Brekelmans, W.A.M. and Baaijens, F.P.T., 2001. An approach to micromacro modeling of heterogeneous materials. *Comput. Mech.* **27(1)**:37-48.
- [7] Miehe, C., Schröder, J. and Schotte, J., 1999. Computational homogenization analysis in finite plasticity Simulation of texture development in polycrystalline materials. *Comput. Methods Appl. Mech. Engrg.* **171**:387-418.
- [8] Chung, P.W., Tammaa, K.K. and Namburub, R.R., 2001. Asymptotic expansion-homogenization for heterogeneous media: computational issues and applications. *Composites Part A*. **32**:1291-1301.
- [9] Fish, J. and Wagiman, A., 1992. Multi-scale finite element method for a periodic and nonperiodic heterogeneous medium. *Adaptive, Multilevel Hierarchical Comput. Strategies ASME-AMD*. **157**:95-117.
- [10] Fish, J., Shek, K., Pandheeradi, M. and Shephard, M.S., 1997. Computational plasticity for composite structures based on mathematical homogenization: Theory and practice. *Comput. Methods Appl. Mech. Engrg.* **15**:53-73.
- [11] Ghosh, S., Lee, K. and Moorthy, S., 1995. Multiple scale analysis of heterogeneous elastic structures using homogenization theory and Voronoi cell finite element method. *Int. J. Solids and Structures*. **32**:27-62.
- [12] Ghosh, S., Lee, K. and Moorthy, S., 1996. Two scale analysis of heterogeneous elastic-plastic materials with asymptotic homogenization and Voronoi cell finite element model. *Comput. Methods Appl. Mech. Engrg.* **132**:63:116.
- [13] Fish, J., Chen, W. and Li, R., 2007. Generalized mathematical homogenization of atomistic media at finite temperatures in three dimensions. *Comput. Methods Appl. Mech. Engrg.* **196**:908-922.
- [14] Feyel, F., 2003. A multilevel finite element method (FE2) to describe the response of highly non-linear structures using generalized continua. *Comput. Methods Appl. Mech. Engrg.* **192**:3233-3244.
- [15] Foresta, S., Pradelb, F. and Sabb, K., 2001. Asymptotic analysis of heterogeneous Cosserat media. *Int. J. Solids and Structures*. **38**:4585-4608.
- [16] Van Der Sluis, O., Vosbeek, P.H.J., Schreurs, P.J.G. and Meijer, H.E.H., 1999. Homogenization of heterogeneous polymers. *Int. J. of Solids and Structures*. **25**:3193-3214.
- [17] Li, X., Liu, Q. and Zhang, J., 2010. A micromacro homogenization approach for discrete particle assembly Cosserat continuum modeling of granular materials. *Int. J. of Solids and Structures*. **47**:291-303.
- [18] Cusatis, G., Pelessone, D. and Mencarelli, A., 2011. Lattice Discrete Particle Model (LDPM) for failure behavior of concrete. I: Theory. *Cement and Concrete Composites*. **33**:881-890.
- [19] Cusatis, G., Mencarelli, A., Pelessone, D. and Baylot, J., 2011. Lattice Discrete Particle Model (LDPM) for failure behavior of concrete. II: Calibration and validation. *Cement and Concrete Composites*. **33**:891-905.

- [20] Cundall, P.A. and Strack, O.D.L., 1979. A discrete element model for granular assemblies. *Geotechnique*. **29(1)**:47-65.
- [21] Tavaréz, F.A. and Plesha, M.E., 2007. Discrete element method for modelling solid and particulate materials. *Int. J. Numer. Meth. Engng.* **70**:379-404.
- [22] Ghaboussi, J. and Barbosa, R., 1990. Three-dimensional discrete element method for granular materials. *International Journal for Numerical and Analytical Methods in Geomechanics* **14**:451-472.
- [23] Hrennikoff, A., 1941. Solution of problems of elasticity by the framework method. *J Appl Mech.* **12**:169-75.
- [24] Burt, N.J. and Dougill, J.W., 1977. Progressive failure in a model heterogeneous medium. *ASCE J Engng Mech Div.* **103**:365-76.
- [25] Hermann, H.J. and Roux. S., 1992. Statistical models for the fracture of disordered media. *Elsevier Science*.
- [26] Bazant, Z.P., Tabbara, M.R., Kazemi, M.T. and Pijaudier-Cabot, G., 1990. Random particle model for fracture of aggregate or fiber composites. *ASCE J Engng Mech.* **116**:1686-705.
- [27] Karihaloo, B.L., Shao, P.F. and Xiao, Q.Z., 2003. Lattice modelling of the failure of particle composites. *Engineering Fracture Mechanics.* **70**:2385-2406.
- [28] Cusatis, G., Bazant, Z. and Cedolin, L., 2003. Confinement-Shear Lattice Model for Concrete Damage in Tension and Compression: I. Theory. *J. Eng. Mech.* **129(12)**:1439-1448.
- [29] Cusatis, G., Bazant, Z. and Cedolin, L., 2003. Confinement-Shear Lattice Model for Concrete Damage in Tension and Compression: II. Computation and Validation. *J. Eng. Mech.* **129(12)**:1449-1458.
- [30] Gitman, I.M., Askes, H. and Sluys, L.J., 2007. Representative volume: Existence and size determination. *Engineering Fracture Mechanics.* **74**:2518-2534.